Cellular and Molecular Life Sciences (2023) 80:5
https://doi.org/10.1007/s00018-022-04642-2

ORIGINAL ARTICLE

LncRNA LENGA acts as a tumor suppressor in gastric cancer through BRD7/TP53 signaling

Shuchun Li[1,3] · Jing Sun[1,2] · Junjun Ma[1,2] · Cixiang Zhou[3] · Xiao Yang[1,2] · Sen Zhang[1,2] · Ling Huang[1,2] · Hongtao Jia[1,2] · Yanfei Shao[1,2] · Enkui Zhang[1,2] · Minhua Zheng[1,2] · Qian Zhao[3] · Lu Zang[1,2]

Received: 2 June 2022 / Revised: 1 November 2022 / Accepted: 22 November 2022 / Published online: 8 December 2022

Abstract

It has been established that long noncoding RNAs (lncRNAs) play a crucial role in various cancer types, and there are vast numbers of long noncoding RNA transcripts that have been identified by high-throughput methods. However, the biological function of many novel aberrantly expressed lncRNAs remains poorly elucidated, especially in gastric cancer (GC). Here, we first identified a novel lncRNA termed LENGA (Low Expression Noncoding RNA in Gastric Adenocarcinoma), which was significantly downregulated in GC tissues compared to adjacent normal tissues. Next, we found that reduced expression of LENGA in GC was also associated with a shorter life expectancy. The proliferation, migration, and invasion of GC cells were increased after LENGA knockdown but restrained after LENGA overexpression in vitro and in vivo. It was further demonstrated that LENGA physically binds to BRD7 (bromodomain-containing 7) in the bromodomain domain and acts as a scaffold that enhances the interaction between BRD7 and TP53 (tumor protein p53), regulating the expression of a subset of genes in the p53 pathway, including CDKN1A (cyclin-dependent kinase inhibitor 1A) and PCDH7 (protocadherin 7), at the transcriptional level. Consistently, the expression of CDKN1A has a positive correlation with LENGA in GC patients. Taken together, this study uncovers a novel tumor suppressor lncRNA, LENGA, and describes its biological function, molecular mechanism, and clinical significance. This highlights the potential importance of targeting the LENGA/BRD7/TP53 axis in GC treatment.

Keywords Gastric cancer · Long noncoding RNA · BRD7 · p53 pathway

Shuchun Li and Jing Sun contributed equally to this work.

✉ Minhua Zheng
zmhtiger@yeah.net

✉ Qian Zhao
qzhao@shsmu.edu.cn

✉ Lu Zang
zanglu@yeah.net

[1] Department of General Surgery, Ruijin Hospital, Shanghai Jiao Tong University School of Medicine, Shanghai 200025, China

[2] Shanghai Minimally Invasive Surgery Center, Ruijin Hospital, Shanghai Jiao Tong University School of Medicine, Shanghai 200025, China

[3] Department of Pathophysiology, Key Laboratory of Cell Differentiation and Apoptosis of Ministry of Education, Shanghai Frontiers Science Center of Cellular Homeostasis and Human Diseases, Shanghai Jiao Tong University School of Medicine, Shanghai 200025, China

Abbreviations

lncRNA	Long noncoding RNA
GC	Gastric cancer
LENGA	Low Expression Noncoding RNA in Gastric Adenocarcinoma
BRD7	Bromodomain-containing 7
TP53	Tumor protein p53
CDKN1A	Cyclin-dependent kinase inhibitor 1A
STR	Short tandem repeat
GSPs	Gene-specific primers
RIP	RNA immunoprecipitation
SPF	Specific pathogen-free
GEO	Gene Expression Omnibus
TCGA	The Cancer Genome Atlas
NCBI	National Center for Biotechnology Information
RACE	Rapid amplification of cDNA ends
FISH	Fluorescent in situ hybridization
CCK-8	Cell Counting Kit-8
4s1m	4 × Streptavidin-binding RNA aptamer

MS	Mass spectrometry
FL	Full-length
CUT&Tag	Cleavage Under Targets and Tagmentation
GSEA	Gene set enrichment analysis
SWI/SNF	Switch/Sucrose Non-Fermentable complex

Introduction

Gastric adenocarcinoma (gastric cancer, GC) is one of the most prevalent malignancies worldwide, with more than half of GC cases occurring in East Asia [1]. In 2020, over a million new cases and an estimated 769,000 deaths were caused by GC, ranking fifth for incidence and fourth for mortality globally [2]. Despite the fact that great progress has been made in recent decades, patients with advanced gastric cancer usually have a poor prognosis due to metastasis and recurrence [3]. Therefore, further investigation and elucidation of the molecular mechanisms of GC may provide novel therapeutic candidates that are expected to improve patient outcomes.

Long noncoding RNAs (lncRNAs) represent transcripts of more than 200 nucleotides in length but with limited coding potential [4]. Recently, numerous lncRNAs have been identified, but it is difficult to clearly define and categorize their functions. Four general archetypes have been proposed for broadly classifying lncRNA functions, including signals, decoys, guides, and scaffolds [5]. Moreover, emerging evidence has demonstrated that lncRNAs have broad functional roles in hallmarks of cancer [6, 7]. LncRNA dysregulation has been observed in various types of cancer, including GC [8–10]. However, only a small number of lncRNAs have been well identified in terms of their functions and mechanisms in GC, and most of them remain uncharacterized.

In the present study, we describe a novel lncRNA named LENGA (Low Expression Noncoding RNA in Gastric Adenocarcinoma). In GC, LENGA is downregulated, and its levels are negatively correlated with prognosis. Exogenous overexpression of LENGA inhibits the proliferation and metastasis of GC in vitro and in vivo. Regarding the molecular mechanism, LENGA binds bromodomain-containing protein 7 (BRD7), which was reported to be a cofactor that regulates gene transcription [11]. LENGA reinforces the interaction of the BRD7/TP53 complex and is needed for BRD7's function in regulating the expression of target genes at the transcriptional level in GC cells. TP53 is an evolutionarily conserved protein that regulates tumor suppression by preserving genomic integrity, responding to environmental perturbations dynamically, and avoiding malignant transformation [12]. Collectively, in this study, we identified a tumor suppressor lncRNA, LENGA, with biological, mechanistic, and clinical implications for human GC.

Materials and methods

GC patient cohort

Tumors and the adjacent normal gastric tissues were obtained from patients with gastric cancer who underwent gastrectomy at Shanghai Ruijin Hospital (Shanghai, China). The study protocol was in accordance with the guidelines set by the Ethical Committee of Ruijin Hospital. Written informed consent was obtained from all participants in the study. The tumor stage of GC was according to the 8th edition classification Union for International Cancer Control (UICC) classification system. The cohort was stored in liquid nitrogen including 62 tumor tissues and paired adjacent normal tissues. None of these patients had received radiotherapy or chemotherapy prior to surgery.

Cell lines and cell culture

Gastric cancer cell lines (MGC803, AGS) were obtained from the Shanghai Institute of Biochemistry and Cell Biology (SIBCB) cell bank, Chinese Academy of Science (Shanghai, China). All cells were cultured in RPMI 1640 medium supplemented with 10% fetal bovine serum (F2442, Sigma-Aldrich, USA), maintained in a 37℃ incubator with a 5% CO_2 condition. All cells were authenticated via short tandem repeat (STR) profiling in 2019 by Shanghai Biowing Applied Biotechnology Co., Ltd., Shanghai, China. Mycoplasma contamination was not found in any of the cell lines.

5′ and 3′ Rapid Amplification of cDNA Ends (RACE)

5′/3′ RACE was performed following the manufacturer's instruction of the SMARTer RACE 5′/3′ Kit (634,858, TaKaRa Bio., China). Gene-specific primers (GSPs) were designed according to the instructions. In brief, 1 μg of total RNA extracted from MGC803 cells was used for cDNA synthesis. GSPs and universal reverse primers were used for the first-round and nested PCR amplification as indicated. The PCR products were subcloned using the pMD19-T vector (6013,6019, TaKaRa Bio., China) for further sequencing. The complete sequence of LENGA was obtained by the sequence of 5'/3'-RACE fragments. GSPs are listed in Table S4.

RNA fluorescence in situ hybridization (RNA-FISH)

RNA-FISH was performed to investigate the location of LENGA by a Fluorescent in Situ Hybridization Kit (Ribo, Guangzhou, China) according to the manufacturer's instructions. Probes of U6 and 18S (located in the nucleus and cytoplasm, respectively) were used as the positive controls.

LENGA's probes were synthesized according to its full length. After hybridization according to protocols, cells were counterstained with DAPI and visualized using a Nikon A1 confocal laser scanning microscope (Nikon, Japan).

Nuclear and cytoplasmic fractionation

The experimental procedure has been described in detail before [13]. Proteins and RNAs were collected separately. RNase Inhibitor (2313, Takara Bio., China) was used to avoid RNA degradation. Western blotting was used to confirm that subcellular fractionation was successful. RT-PCR was performed to determine the location of LENGA, and U6 and 18S represented nucleus and cytoplasm location, respectively.

Construction of plasmids and cell transfection

Plasmids and/or siRNAs were transfected into cells using Lipofectamine2000 (11668019, Invitrogen, USA) according to the manufacturer's instruction. The siRNAs for LENGA and BRD7 were designed and synthesized by Genepharma (Shanghai, China). Table S4 contains detailed information about the siRNA and siNC sequences. The full-length human LENGA and BRD7 (NM_013263.5) are cloned from complementary DNA (cDNA) in MGC803 cells into the pcDNA3.1 expression vectors. For RNA pull-down assay, the 3′ end of LENGA was fused to 4 × streptavidin-binding RNA aptamer (4s1m) in pcDNA3.1 vector [14]. For exogenous BRD7 RIP and Co-IP, full length BRD7 was cloned to the pCMV-3Tag expression vector (Agilent Technologies, US). In order to establish cell line with stable BRD7 knockdown, shBRD7 lentivirus were constructed by Genepharma (Shanghai, China). Stable shBRD7 transfectants were selected in complete medium containing 1 μg/mL puromycin.

Cell growth and proliferation assay

Cell proliferation was assessed by Cell Counting Kit-8 (Dojindo, Japan). Briefly, differently treated cancer cells were seeded into 96 well plates at an initial 2000 cells/100 μL per well. CCK-8 (10 μL/well) was added to cells every 24 h. Then after 2 h of incubation under 37 °C, the absorption value in 450 nm was detected by spectrophotometer.

Cell colony formation assay

Suspend the cells in the culture medium. The cells are then seeded in 6 well plates in triplicate (500–1000 cells/well) and maintained in the incubator. Change the medium every 3 days. After culture for about 2 weeks, when colonies are visible under a microscope, stop culture and wash with PBS. Then fix colonies with methanol for 30 min, and stain with crystal violet for 20 min. Software ImageJ (https://imagej.nih.gov/ij/) can be used for colony counting.

Cell migration and invasion assay

Trans-well assay was used to determine the cell migration and invasion ability. For migration assay, cells suspended in serum-free RPMI 1640 were seeded into the upper chambers (3422, 8 μm pore size, Corning, USA). The lower chamber contained the medium supplemented with 10% FBS After 24 h of incubation, the filters were fixed in methanol and stained with 0.05% crystal violet. The upper faces of the filters were gently scratched to make sure all cells that migrated across the membrane were counted. In the invasion assays, the upper chambers were coated with Matrigel (356234, Corning, USA) before adding the cells to the chambers. Triplicates of these experiments were performed, and data were collected for further analysis.

RNA pull-down assay

Plasmids expressing full-length LENGA containing 4s1m tagged [14], as well as control vector were transfected into MGC803 cells using Lipofectamine 2000 (11668, Thermo Fisher Scientific). Cells were collected after 3 days and washed with PBS. Then cells were suspended in lysis buffer containing RNase Inhibitor (2313A, Takara, Japan), Cocktail (539134, Millipore, USA), and PMSF (ST506, Beyotime, China). After centrifuging, 50μL supernatant was reserved as an input sample and the rest of the supernatant was transferred to 1.5 mL EP tubes incubated with Streptavidin Magnetic Beads (S1420, New England Bio., USA) at 4℃ for overnight, and then washed with cold wash-buffer for 6 times. Finally, the precipitate was collected using a magnet. To release the proteins, 50 μL 2 × SDS electrophoresis sample buffer was added to the precipitate as RNA pulldown samples. The entire lysates were analyzed using mass spectrometry (MS) or western blotting. MS was performed at the Core Facility of Basic Medical Sciences, Shanghai Jiao Tong University School of Medicine.

RNA immunoprecipitation (RIP) assay

Firstly, to crosslink proteins and RNA, 540 μl of 37% formaldehyde was added to a 15 cm dish containing 20 mL medium, incubating for 10 min at room temperature. Subsequently, 2 mL 1.25 M glycine was added to the medium. Then, over 10^7 cells were collected and lysed in 100 μL RIP lysis buffer (150 mM KCL, 25 mM Tris (pH 7.4), 5 mM EDTA, 0.5%NP40, 1 mM PMSF, 1 mM DTT, 1% Cocktail, 200 U/mL RNase inhibitor). After centrifuge at 4 °C

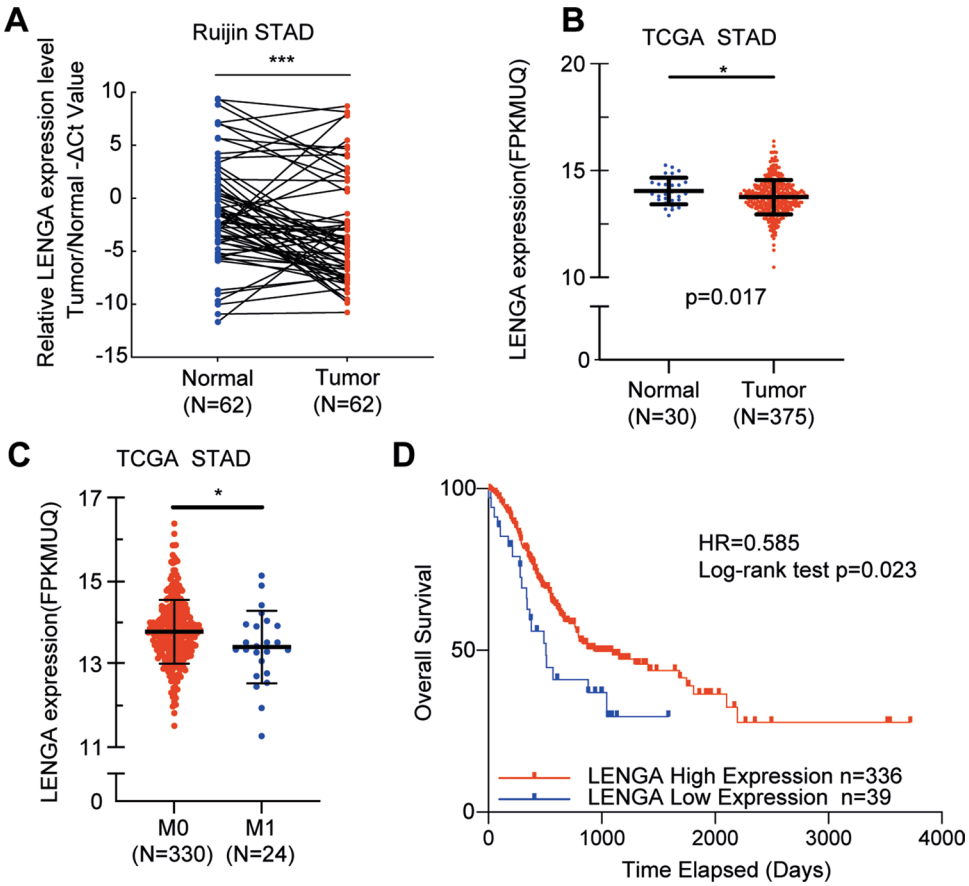

Fig. 1 LENGA expression is significantly downregulated in GC samples and associated with a better prognosis. **A** Quantitative Rt-PCR detection of LENGA expression levels in 62 GC patients and 62 normal controls. The paired t-test was used to compare the difference in tumor and normal groups. **B** Statistical analysis of LENGA expression in the primary tumor ($n=375$) and normal ($n=30$) samples from TCGA-STAD. **C** Statistical analysis of LENGA expression in GC tissues with distant metastasis (M1, $n=24$) and without distant metastasis (M0, $n=330$) from TCGA-STAD. **D** Kaplan–Meier curve depicting the overall survival of patients with high ($n=336$) or low ($n=39$) levels of LENGA in the TCGA-STAD cohort. $^{*}P<0.05$, $^{**}P<0.01$, $^{***}P<0.001$

for 10 min at 12,000*g*, the supernatant was incubated with Protein A/G PLUS-Agarose (sc-2003, Santa Cruz, USA) conjugated with BRD7 antibody (ab56036, Abcam, USA), ANTI-FLAG M2 Affinity Gel (A2220, Sigma, USA), mouse IgG (sc-2025, Santa Cruz, USA) or rabbit IgG (B900610, Proteintech, China) for 5 h. Then, the precipitation was washed 6 times with wash buffer (50 mM Tris–HCl (pH 7.4), 150 mM NaCl, 2 mM EDTA, 0.05% NP40, 1 mM DTT, Cocktail, and RNase inhibitor). Finally, RNA coupled with agarose beads was extracted using TRIzol reagent (Invitrogen, 15596026, USA) and detected by RT-PCR.

Western blotting

In brief, total proteins were extracted from cells by 1 × SDS loading buffer with protease inhibitors (Beyotime, China). Western blotting was conducted according to the previously described [15]. The antibodies used in this study are described in detail in Supplementary Table S5. The signals were visualized using an ECL detection reagent (Millipore). Western blotting images were captured by Tanon 5200 imaging system (Tanon, China).

RNA extraction and quantitative real-time PCR

Total RNA was extracted using TRIzol reagent (15596026, Invitrogen, USA) following the manufacturer's protocol. The cDNA synthesis was performed with a Reverse Transcription System (KR118, TIANGEN, China). The mRNA levels were detected using Power SYBRGreen PCR Master Mix (4367659, ABI, USA) and an ABI QuantStudio 5 Real-Time PCR System (ABI, USA). Each sample had three repetitions. The relative expression of the mRNA levels was normalized to ACTB and calculated relative expression by the $2^{-\Delta\Delta Ct}$ method. The RT-PCR primers, synthesized by Genewiz Biological Technology (Genewiz, Suzhou, China) are shown in Supplementary Table S4.

Coimmunoprecipitation (Co-IP)

Coimmunoprecipitation was performed as follows: briefly, cells were collected and lysed in RIPA lysis buffer (P0013D, Beyotime, China) with Cocktail (539134, Millipore, USA), and PMSF (ST506, Beyotime, China). The precleared lysates were collected and incubated with rabbit anti-BRD7 (ab56036, Abcam, USA) agarose conjugate, ANTI-FLAG M2 Affinity Gel (A2220, Sigma, USA), mouse IgG (sc-2025, Santa Cruz, USA) agarose conjugate or rabbit IgG

Table 1 Association of LENGA expression with clinicopathological parameters

Characteristics	LENGA expression		
	High ($n=18$)	Low ($n=44$)	Chi-squared test P value
Age (years)			0.274
< 60	7 (38.9%)	11 (61.1%)	
≧ 60	11 (25.0%)	33 (75.0%)	
Gender			0.769
Male	12 (27.9%)	31 (30.5%)	
Female	6 (31.6%)	13 (68.4%)	
Tumor size			0.055
≦5.5	13 (39.4%)	20 (60.6%)	
> 5.5	5 (17.2%)	24 (82.8%)	
Histologic differentiation			**0.033**
Poorly	7 (18.9%)	30 (81.1%)	
Well/moderately	11 (44.0%)	14 (56.0%)	
Bormann classification			0.221[a]
1	1 (14.3%)	6 (85.7)	
2	10 (25.0%)	30 (75.0%)	
3	5 (41.7%)	7 (58.3%)	
4	2 (66.7%)	1 (33.3%)	
Invasion depth			0.763[a]
T1	0 (0.0%)	4 (100.0%)	
T2	1 (33.3%)	2 (66.7%)	
T3	4 (28.6%)	10 (71.4%)	
T4	13 (31.7%)	28 (68.3%)	
Lymphatic node stage			**0.010[a]**
N0	2 (15.4%)	11 (84.6%)	
N1	0 (0.0%)	6 (100.0%)	
N2	8 (66.7%)	4 (33.3%)	
N3	8 (25.8%)	23 (74.2%)	
Positive LNs			**0.025[a]**
≦15	17 (36.2%)	30 (63.8%)	
> 15	1 (6.7%)	14 (93.3%)	
Vessels invasive			0.720
No	7 (31.8%)	15 (68.2%)	
Yes	11 (27.5%)	29 (72.5%)	
Nervus invasive			0.954
No	6 (28.6%)	15 (71.4%)	
Yes	12 (29.3%)	29 (70.7%)	
Distant metastasis			0.710[a]
M0	18 (29.5%)	43 (70.5%)	
M1	0 (0.0%)	1 (100.0%)	
TNM stage			0.512[a]
I	1 (16.7%)	5 (83.3%)	
II	1 (11.1%)	8 (88.9%)	
III	16 (34.8)	30 (65.2%)	
IV	0 (0.0%)	1 (100.0%)	
CA19-9			0.186
High	5 (45.5%)	6 (54.5%)	
Normal	13 (25.5%)	38 (74.5%)	
CEA			0.877
Normal	14 (28.6%)	35 (71.4%)	
High	4 (30.8%)	9 (69.2%)	
Ki67			0.274
≦65	7 (38.9%)	11 (61.1%)	
> 65	11 (25.0%)	33 (75.0%)	
Her2			0.444
Negative	8 (34.8%)	15 (65.2%)	
Positive	10 (25.6%)	29 (74.4%)	

The bold value indicates it has statistical difference between two groups for the characteristic

[a]Fisher's Exact Test

(B900610, Proteintech, China) agarose conjugate overnight at 4 °C. Then the precipitate was washed several times with wash buffer and resuspended in loading buffer, boiled over 100 °C for 10 min for Western blot analysis.

Xenograft model

All animal experimental protocols are approved by the Institutional Animal Use and Care Committee of Shanghai Jiao Tong University School of Medicine. Four-week-old BALB/c nude male mice were housed under specific pathogen-free (SPF) conditions. A total of 5×10^6 MGC803 cells, suspended in about 100 μL PBS, with different treatments were injected subcutaneously into nude mice. Xenograft tumor was measured every 7 days. 3 or 4 weeks after injection, all the mice were sacrificed, while the harvested tumors were weighed and measured.

Transcriptome sequencing and bioinformatic analysis

Differential gene expression analysis of mRNA was performed between LENGA siRNA or siNC MGC803 cells. Transcriptome sequencing was performed by Cloud-Seq Biotech (Shanghai, China). RNA libraries were constructed by rRNA-depleted RNAs with TruSeq Stranded Total RNA Library Prep Kit (Illumina, USA). Library sequencing was performed on the Illumina Hiseq 4000 sequencer with 150 bp paired-end reads. After adaptor-trimming and low-quality reads removal by cutadapt software (v1.9.3)[16], the high-quality clean reads were aligned to the reference genome with hisat2 software (v2.0.4) [17]. Then, according to the Ensembl's gene annotation file, cuffdiff software (part of cufflinks [18]) was used to get the gene level FPKM as the

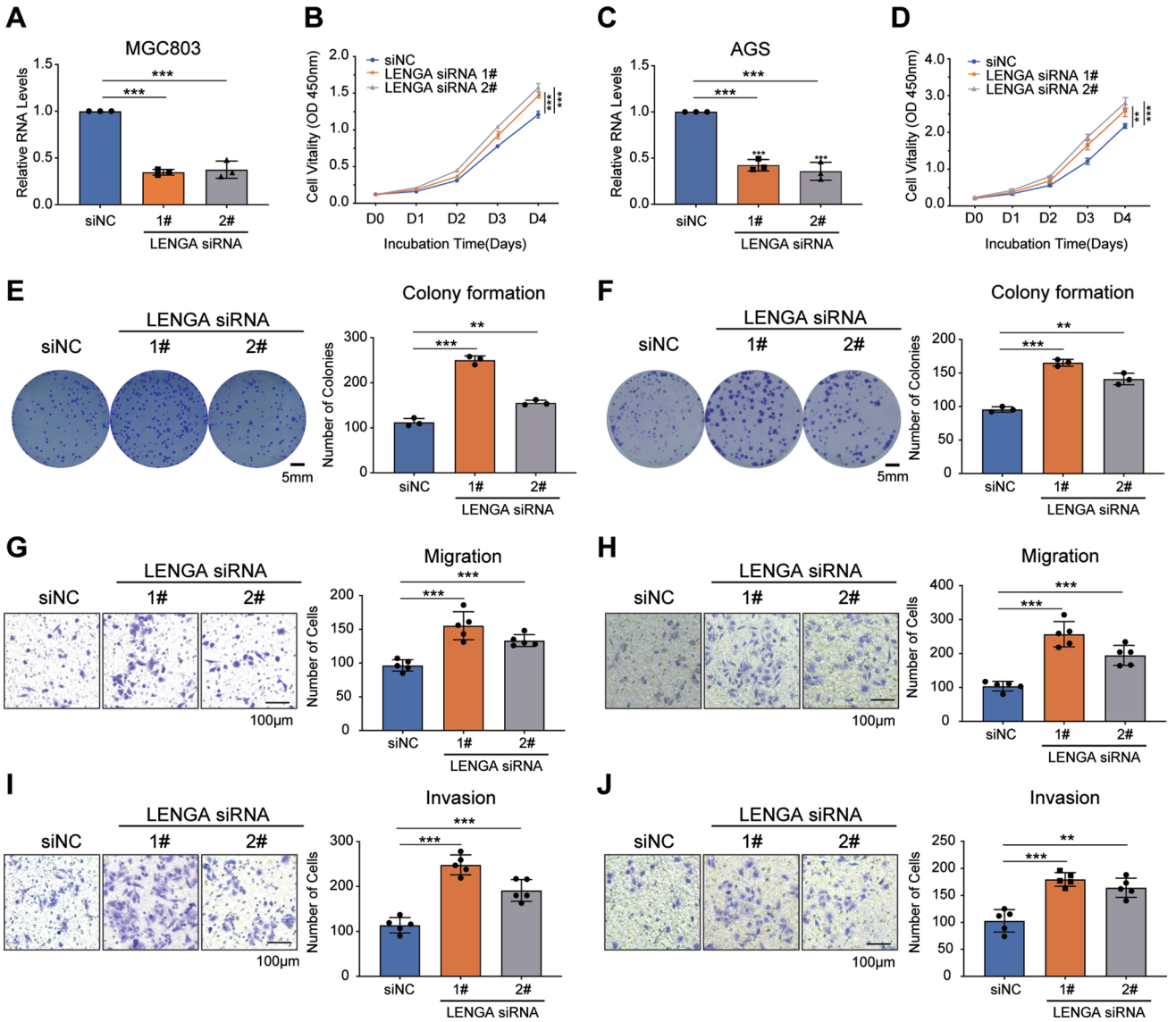

Fig. 2 LENGA knockdown promotes GC cell growth and metastasis in vitro. **A**, **C** Rt-PCR analyzed LENGA expression in MGC803 (**A**) and AGS (**C**) transfected with siNC or LENGA siRNA 1/2#. **B**, **D** CCK-8 assay was used to detect the cell proliferation in MGC803 and AGS after different treatments. **E**, **F** Colony formation assays were performed to determine the growth in LENGA siRNA transfected cells. **G–J** Trans-well assays were used to determine the migration (**G**, **H**) and invasion (**I**, **J**) when LENGA knockdown. Representative images of every assay were shown. The date represents the mean ± SD from three independent experiments. If applicable, statistical analyses were presented on the right panel of each figure. $^{*}P<0.05$, $^{**}P<0.01$, $^{***}P<0.001$

expression profiles of mRNA, and fold change and p-value were calculated based on FPKM, differentially expressed mRNA were identified. GO and Pathway enrichment analyses were performed based on the differentially expressed mRNAs. Other bioinformatics analyses were performed as default, including Gene Set Enrichment Analysis using GSEA v3.0 (http://www.broadinstitute.org/gsea/), Metascape [19], and Ingenuity Pathway Analysis (IPA, Qiagen). The data were deposited to the NCBI's GEO Repository.

CUT&Tag for quantifying DNA enrichment

CUT&Tag assay was performed according to Prof. Henikoff et al. described [20, 21] with NovoNGS CUT&Tag High-Sensitivity Kit (N259-YH01, Novoprotein, Shanghai, China). It is a relatively new technique investigating interactions between proteins and DNA, which is similar to chromatin immunoprecipitation (ChIP) assay but more efficient, convenient, and exceptionally low background. Briefly, treated cells were washed and incubated with Concanavalin A coated magnetic beads. Then cells were resuspended

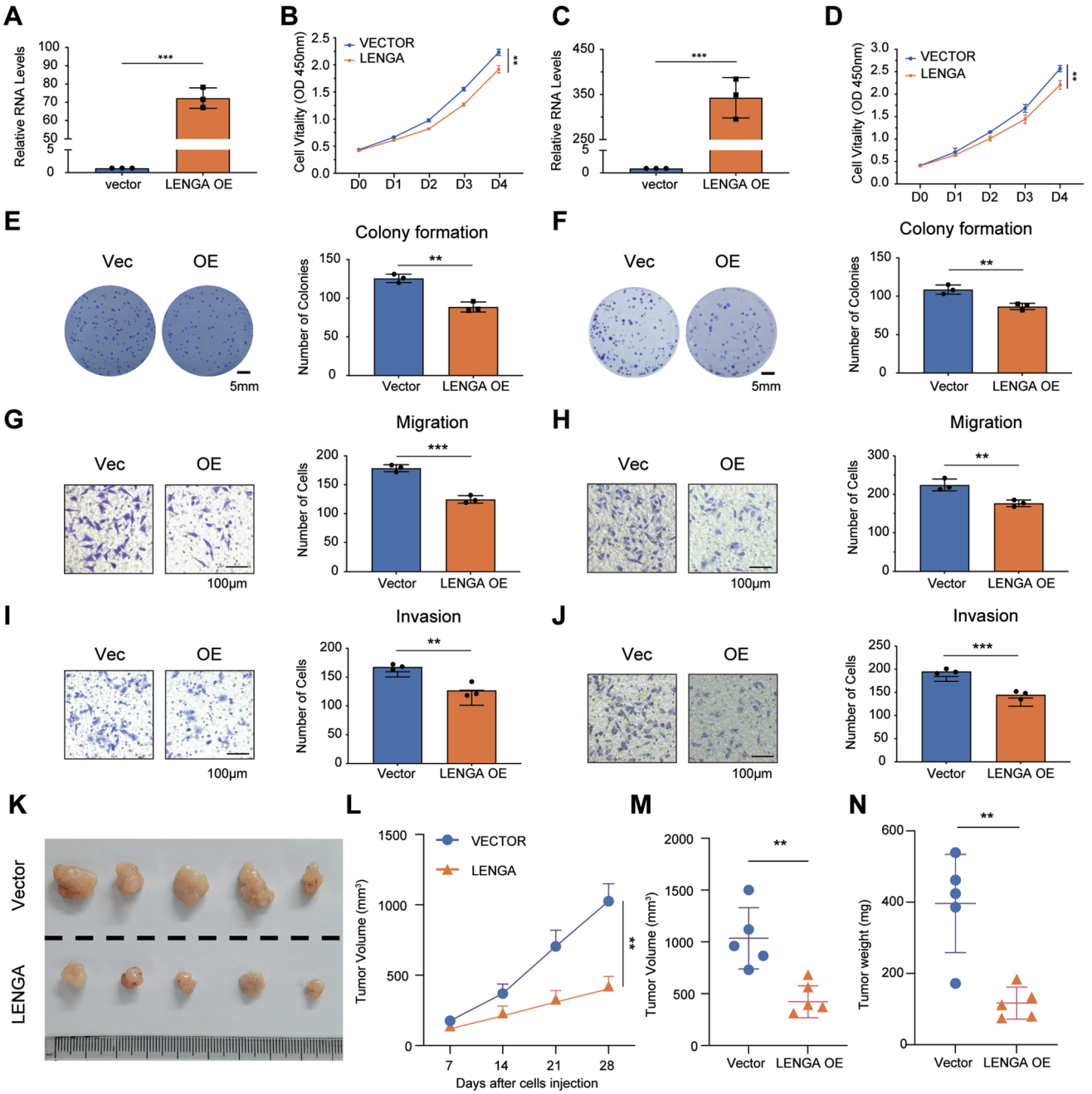

Fig. 3 LENGA overexpression inhibits GC cell growth and metastasis in vitro and in vivo. **A**, **C** Rt-PCR analyzed LENGA expression in MGC803 (**A**) and AGS (**C**) transfected with LENGA overexpression plasmid (OE) or empty vector (pcDNA3.1). **B**, **D** CCK-8 assay was used to detect the cell proliferation in MGC803 and AGS after different treatments. **E**, **F** Colony formation assays were performed to determine the growth in LENGA-OE cells. **G–J,** Trans-well assays were used to determine the migration (**G**, **H**) and invasion (**I**, **J**) in LENGA-OE cells. **K** Morphological observation of tumors formed after injection of nude mice with MGC803 cell lines with LENGA-OE. **L–N** Tumor volume (**L**, **M**), and tumor weight (**N**) were used to evaluate the xenograft tumor. Representative images of every assay were shown. The date represents the mean ± SD from three independent experiments. If applicable, statistical analyses were presented on the right panel of each figure. $^{*}P < 0.05$, $^{**}P < 0.01$, $^{***}P < 0.001$

with primary BRD7 antibody (Abcam, USA) (1:50 dilution in Primary Antibody Buffer) or control IgG, and rotated for 2 h at room temperature. Then, incubated with secondary antibody and ChiTag 2.0 Transposome, subsequently. Next, cells were resuspended in Tagmentation Buffer and incubated at 37 °C, and DNA fragments were extracted with TIANSeq Size Selection DNA Beads (NG316, TIANGEN, China). Finally, library construction was performed

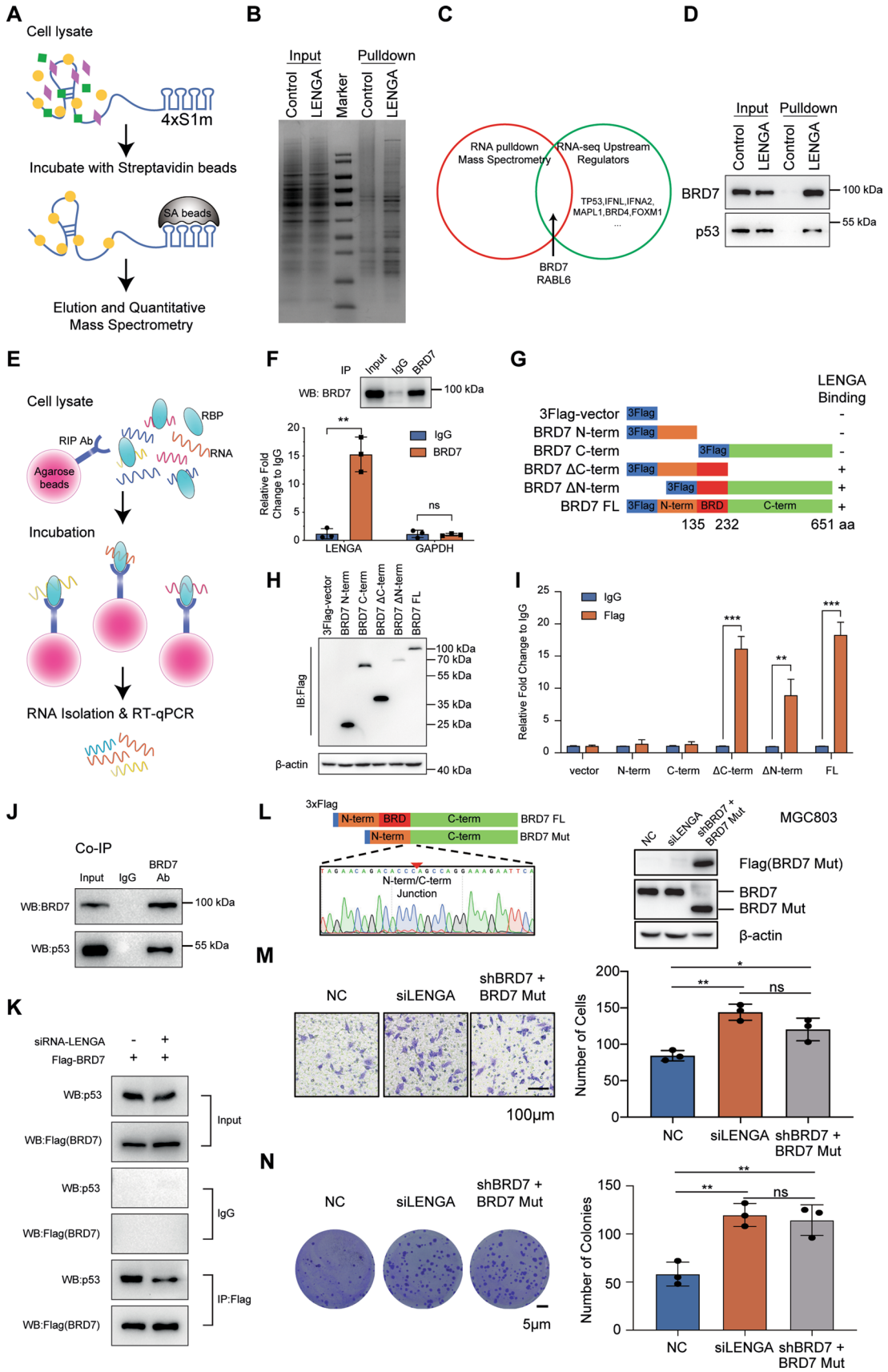
A
Cell lysate
4xS1m
Incubate with Streptavidin beads
SA beads
Elution and Quantitative Mass Spectrometry
B
Input
Pulldown
Control
LENGA
Marker
Control
LENGA
C
RNA pulldown Mass Spectrometry
RNA-seq Upstream Regulators
TP53,IFNL,IFNA2, MAPL1,BRD4,FOXM1 ...
BRD7
RABL6
D
Input
Pulldown
Control
LENGA
Control
LENGA
BRD7
100 kDa
p53
55 kDa
E
Cell lysate
RBP
RIP Ab
RNA
Agarose beads
Incubation
RNA Isolation & RT-qPCR
F
IP
Input
IgG
BRD7
WB: BRD7
100 kDa
Relative Fold Change to IgG
IgG
BRD7
ns
LENGA
GAPDH
G
LENGA Binding
3Flag-vector
BRD7 N-term
BRD7 C-term
BRD7 ΔC-term
BRD7 ΔN-term
BRD7 FL
3Flag
N-term
BRD
C-term
135
232
651 aa
H
3Flag-vector
BRD7 N-term
BRD7 C-term
BRD7 ΔC-term
BRD7 ΔN-term
BRD7 FL
IB:Flag
100 kDa
70 kDa
55 kDa
35 kDa
25 kDa
β-actin
40 kDa
I
IgG
Flag
Relative Fold Change to IgG
vector
N-term
C-term
ΔC-term
ΔN-term
FL
J
Co-IP
Input
IgG
BRD7 Ab
WB:BRD7
100 kDa
WB:p53
55 kDa
K
siRNA-LENGA
Flag-BRD7
WB:p53
WB:Flag(BRD7)
Input
WB:p53
WB:Flag(BRD7)
IgG
WB:p53
WB:Flag(BRD7)
IP:Flag
L
3xFlag
N-term
BRD
C-term
BRD7 FL
BRD7 Mut
N-term/C-term Junction
NC
siLENGA
shBRD7 + BRD7 Mut
MGC803
Flag(BRD7 Mut)
BRD7
BRD7 Mut
β-actin
M
NC
siLENGA
shBRD7 + BRD7 Mut
100μm
Number of Cells
NC
siLENGA
shBRD7 + BRD7 Mut
N
NC
siLENGA
shBRD7 + BRD7 Mut
5μm
Number of Colonies
NC
siLENGA
shBRD7 + BRD7 Mut

◂**Fig. 4** LENGA interacts with BRD7 and strengthens the combination of BRD7 with TP53. **A** Schematic of RNA pull-down assay, which identifies the LENGA-associated cellular interactors. Full length of LENGA with 4s1m was transfected into GC cells, and streptavidin beads were incubated with total cell lysates. **B** Coomassie brilliant blue G-250 dye showed the LENGA-associated cellular proteins. **C** The Venn diagram showed the candidate proteins which interacted with LENGA. The red section of the Venn diagram represents the proteins identified by MS in the RNA pull-down assay. The green section of the Venn diagram represents upstream regulators, derived from IPA analysis for LENGA knockdown transcriptome (RNA) sequencing. **D** Western blot using the indicated antibodies to verify the interactors of LENGA. **E** Schematic of RNA immunoprecipitation (RIP). **F** Rt-PCR analysis of the levels of LENGA or GAPDH in precipitates of anti-BRD7 antibody RIP (endogenous RIP assay, normalized with the IgG control group). Western blotting confirmed BRD7 was in the precipitate (upper panel). **G** Schematic of deletion mapping of the BRD7-binding regions in LENGA. RIP assay for flag tagged full-length or truncated BRD7 protein (**H**), followed by Rt-PCR assay for LENGA (**I**). The co-IP assay was performed to detect the interaction between BRD7 and TP53 (**J**), and after transfection of LENGA siRNA (**K**). **L** Schematic and western blotting analysis of BRD domain deletion of BRD7 (BRD7 Mut). Trans-well (**M**) and Colony formation (**N**) assays were used to determine the motility and growth. $*P<0.05$, $**P<0.01$, $***P<0.001$

according to the manufacturer's instructions with 17 cycles of PCR. Prior to the library sequencing, quality control of each library was made by Bioanalyzer (Agilent 2100 Bioanalyzer, USA). Libraries were sequenced on a combination of Illumina instruments (PE150, Nova-seq) by GENEWIZ, Suzhou, China.

For analysis, reads were filtered for quality and aligned with bowtie2 (v2.3.0) against the Homo sapiens (hg38) genome. Following filtering, alignment reads with sambamba (v0.7.1) and samtools (v1.9). Next, MACS2 (v2.2.6) [22] was used for calling peaks. Visualization of peaks along genomic regions of interest was performed with IGV (v2.11.1). ChIPseeker (v1.22.1) was used for peak annotation. The heatmap and profile of genes with a peak within 3 kb of TSS were visualized by deepTools (v3.3.0) [23].

Public datasets collection

Human LncRNA microarray (Arraystar Human LncRNA V3.0) for GC and normal adjacent tissues were downloaded from the NCBIs Gene Expression Omnibus (GEO, GSE99417). The datasets GSE99417 consisted of 6 paired GC and adjacent tissues. We reanalyzed the dataset to identify the potential lncRNAs and explore their biological functions. Then, candidate lncRNAs' expression levels were validated by The Cancer Genome Atlas (TCGA) database. TCGA RNA-seq and clinical data were downloaded from the UCSC Xena platform (https://xenabrowser.net/). Additionally, the ChIP-seq datasets for H3K9ac, H3K4me3, and H3K27ac in HeLa-S3 and A549 were obtained from ENCODE/Broad Institute in order to integrate the analysis of the binding site of BRD7 with their own data [24]. These datasets were downloaded from GEO (GSE29611).

Statistical analysis

All in vitro experiments were repeated at least in triplicate. Statistical analyses were carried out by SPSS 22.0 (SPSS, USA) and GraphPad Prism 9.0 (GraphPad Software Inc., USA) software. Student's *t* test, Chi-square test, two-way ANOVA, the Kaplan–Meier method, and the log-rank test were used to analyze the data. *P* values <0.05 were considered statistically significant.

Results

LENGA, a novel lncRNA, is identified to be downregulated and is associated with a better prognosis in GC

In order to discover the function of lncRNAs in GC, we reanalyzed the lncRNA microarray [25]. In total, 997 differentially expressed lncRNAs were screened while the filtering criteria were set at FDR <0.001 and $|\log2FC|>2$, with 353 upregulated and 644 downregulated compared with adjacent normal tissue (Fig. S1A, B). Then, we identified the top 85 differentially expressed lncRNAs by a higher level of FDR. Some of them have been reported in GC previously, such as LINC00982 [26], HOXA11-AS [27], and lncRNA UCA1 [28]. For further study, we focused on the novel transcripts that were included in the National Center for Biotechnology Information (NCBI) reference sequence (RefSeq) database (https://www.ncbi.nlm.nih.gov/refseq/) but never studied before, such as LOC105378662 (XR_001737994.1), LINC02447 (NR_027441.1), LOC105369306 (NR_147887.1), and LOC105369881 (XR_945161.1).

Next, we used RT−PCR to verify the aforementioned lncRNA expression in gastric cancer patient tissues. However, due to their very low abundance, some lncRNAs were difficult to detect (Fig. S1C). Finally, we identified LOC105378662, a novel lncRNA, and we named it LENGA (Low Expression Noncoding RNA in Gastric Adenocarcinoma) because it was downregulated in 62 paired human GC tissues compared to normal gastric mucosa (Fig. 1A). Furthermore, we analyzed the correlation between LENGA and the clinical characteristics in the patient cohort from our hospital (Table 1). The low expression of LENGA was positively associated with poorer differentiation in primary tumors and lower lymph node metastasis rates (p values of 0.033 and 0.007, respectively). In addition, TCGA-STAD database showed that the expression of lncRNA LENGA (ENSG00000228436) was significantly lower in STAD

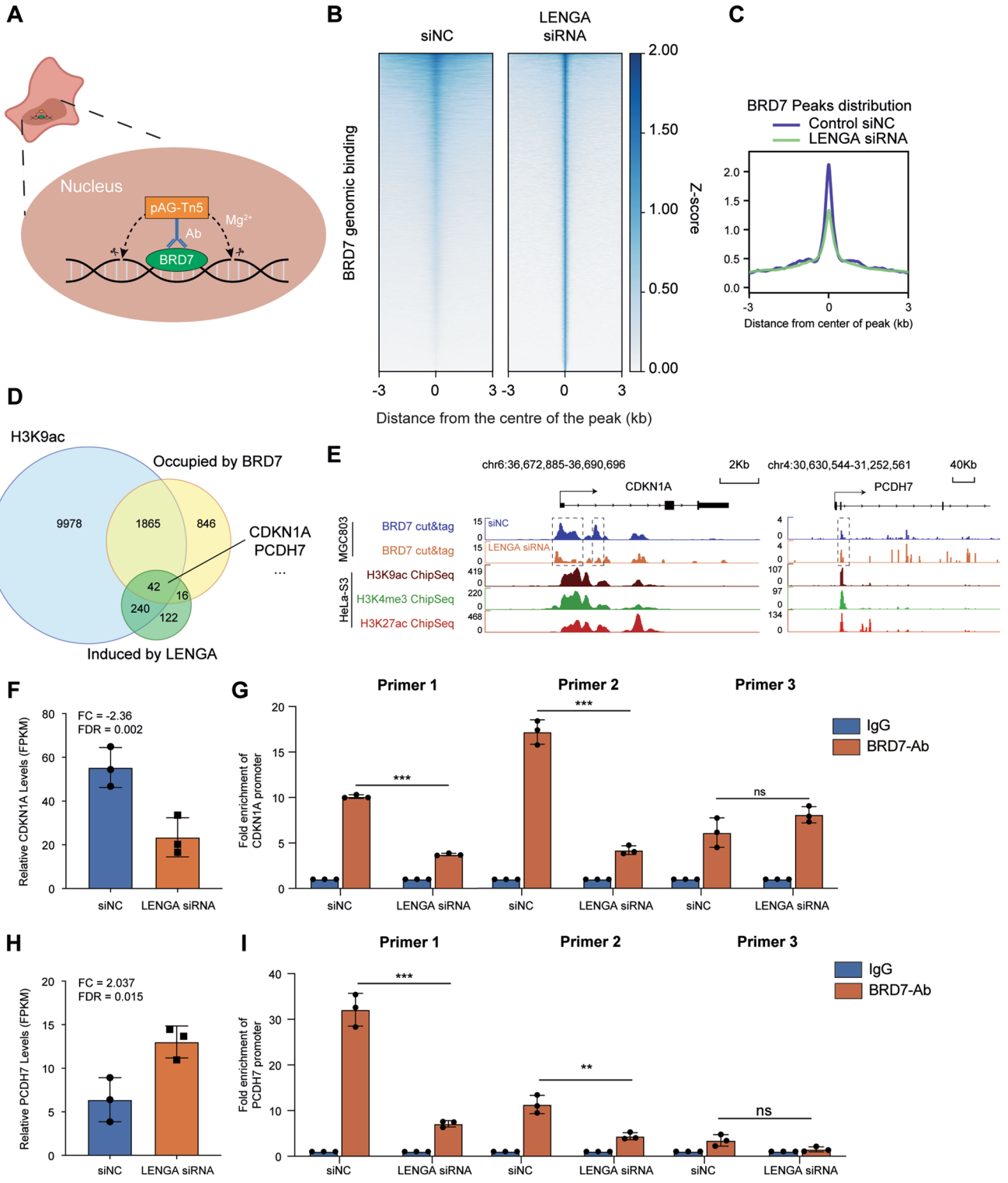

(Fig. 1B). In cases with distant metastasis (M1), the expression of LENGA was lower than that in cases without metastasis (M0) (Fig. 1C). The Kaplan–Meier (K-M) survival curves showed that lncRNA LENGA expression has a significant positive association with a better outcome in these patients (Fig. 1D). Thus, LENGA is downregulated and is associated with a better prognosis in GC.

◂**Fig. 5** LENGA co-localized with BRD7 genome-wide. **A** Schematic of CUT&Tag, digesting targeted chromatin fragments by the protein-A/G-Tn5 transposase, and transposing specific adaptors to the end of DNA fragments. Magnesium (Mg^{2+}) is required for enzymatic activity. The arrows indicate sites of DNA cleavage by transposase. **B**, **C** Heatmaps, and profile plots showed BRD7 global genomic binding at the target sites in MGC803 cells after the transduction of siNC and LENGA siRNA. **D**, Blue, yellow, and green represent genes that are modified by H3K9ac, occupied by BRD7, and differentially expressed when LENGA knockdown, respectively. The intersection were the genes regulated by these three factors. **E**, Representative genes regulated by BRD7 and LENGA simultaneously, such as CDKN1A. The dotted box indicates the region of differential peaks in siNC and LENGA siRNA. The expression level of CDKN1A (**F**) and PCDH7 (**H**) in RNA-seq. **G**, **I** CUT&Tag followed by PCR was performed to quantify the enrichment of BRD7 at CDKN1A and PCDH7 promoter regions. $*P<0.05$, $**P<0.01$, $***P<0.001$

Characterization of the lncRNA LENGA

LENGA is located on chromosome 1p34. Since it had never been reported before, we analyzed its sequence first. We determined the transcriptional initiation and termination sites of LENGA by RACE. The RACE primers were designed according to the sequence of XR_001737994.1, avoiding overlap with its antisense strand coding gene RHBDL2 (Fig. S2A). As shown in Fig. S2D, the full length of LENGA is 873 bp, almost twice as long as the predicted sequences (XR_001737994.1 442 bp), and it was transcribed with a poly(A) tail. To confirm that LENGA did not have the ability to encode proteins, bioinformatics software was used to predict the coding potential of LENGA. The Coding Potential Assessing Tool (CPAT) [29] showed that LENGA's coding probability was 0.10, but it was 1.00 for NM 002046.7 (*GAPDH* mRNA) and NM 001101.5 (*ACTB* mRNA) (Fig. S2E). Open Reading Frame Finder (ORFfinder, https://www.ncbi.nlm.nih.gov/orffinder) could not search for any potential protein-encoding segments in LENGA (Fig. S2F). These results revealed that LENGA had very weak protein-coding potential.

Furthermore, since the cellular locations of lncRNAs are often associated with their biological function [6], we synthesized RNA fluorescent in situ hybridization (FISH) probes for LENGA, U6 (almost expressed in the nucleus), and 18S (almost expressed in the cytoplasm). The RNA FISH test in MGC803 cells showed that LENGA was mainly located in the nucleus (Fig. S3A), which was confirmed by the nuclear and cytoplasmic subcellular fraction assay (Fig. S3B-C).

LENGA, a candidate tumor suppressor lncRNA, inhibits both GC proliferative and metastatic capacities in vitro and in vivo

To elucidate whether LENGA plays a role in GC tumorigenesis, LENGA was knocked down by transfection with two different short-interfering RNAs (siRNA 1# and siRNA 2#) and control siRNA (siNC) (Fig. 2A, C). The Cell Counting Kit-8 (CCK-8) and colony formation assays showed that LENGA silencing enhanced cell growth capability in human MGC803 and AGS GC cell lines (Fig. 2B, D–F). Moreover, the knockdown of LENGA dramatically improved the migration and invasion abilities of the above cell lines (Fig. 2G–J). In the gain-of-function assay, we overexpressed LENGA in MGC803 and AGS cells with plasmid transduction, leading to 75-fold and 350-fold increases in LENGA levels intracellularly, respectively (Fig. 3A, C). Contrary to LENGA knockdown, the effect of cell proliferation (Fig. 3B, D) and colony formation abilities (Fig. 3E, F) were abolished in the LENGA overexpression (LANGA-OE) group compared with the respective vector controls in both cell lines. Additionally, LENGA-OE significantly inhibited the migration and invasion of MGC803 and AGS cells (Fig. 3G–J).

To further validate the phenomena observed in vitro, a xenograft mouse tumor model was used to determine the function of LENGA in vivo. The results showed that overexpression of LENGA dramatically reduced the tumor growth of MGC803 cells in vivo (Fig. 3K), as demonstrated by the remarkable decrease in the mean volume (Fig. 3L, M) and tumor weight (Fig. 3N) in the LENGA-OE group compared to those in the vector control group. Taken together, LENGA might play a critical role in inhibiting GC cell growth and metastasis.

LENGA interacts with BRD7 and strengthens the binding of BRD7 with TP53

Next, we explored the molecular mechanism by which LENGA arrests GC progression. LncRNAs localized in the nucleus are generally assumed to play a role in regulating gene transcription [30]. An RNA pull-down assay was used to identify potential transcription regulators binding to LENGA. We constructed a plasmid that fused the 3' end of LENGA to 4s1m [14] and transfected it into MGC803 cells. Then, proteins interacting with LENGA can be isolated from the precipitate of cell lysis and streptavidin beads (Fig. 4A). Subsequently, purified proteins were detected by SDS/PAGE with Coomassie brilliant blue G-250 dye (Fig. 4B) and mass spectrometry (MS). MS analysis showed that 128 proteins might interact with LENGA (Table S1). Furthermore, RNA-seq analysis was performed to compare the gene expression profiles of MGC803 cells with LENGA knockdown compared to its negative control. IPA (Ingenuity Pathway Analysis, Ingenuity, Qiagen) upstream regulator analysis was carried out using the RNA-seq expression matrix to predict upstream transcriptional regulators. In total, 55 upstream regulators were found with statistical significance, of which 26 were inhibited and 29 were activated (Table S2). We then took the intersection of MS and

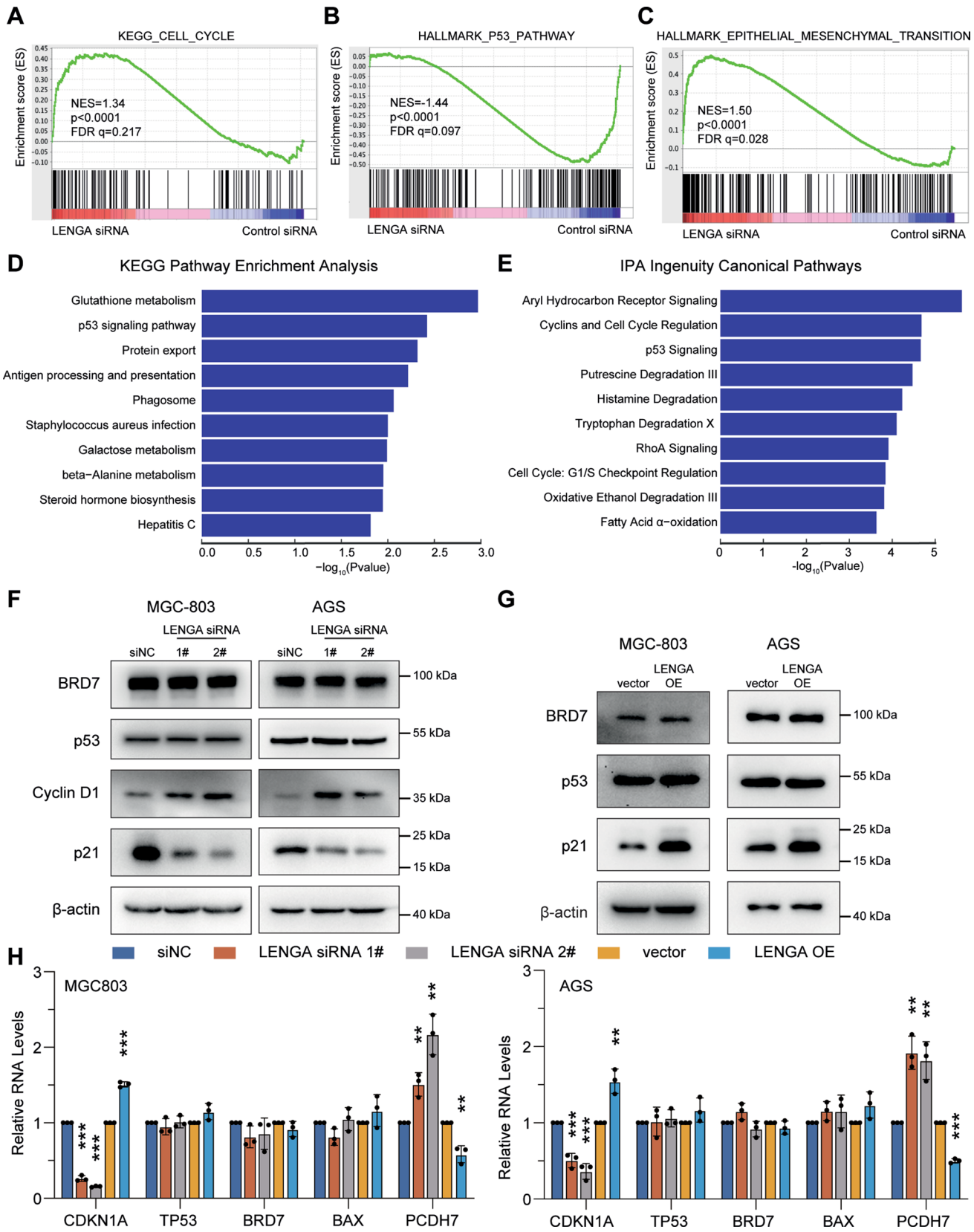
A
KEGG_CELL_CYCLE
Enrichment score (ES)
NES=1.34
p<0.0001
FDR q=0.217
LENGA siRNA
Control siRNA
B
HALLMARK_P53_PATHWAY
Enrichment score (ES)
NES=-1.44
p<0.0001
FDR q=0.097
LENGA siRNA
Control siRNA
C
HALLMARK_EPITHELIAL_MESENCHYMAL_TRANSITION
Enrichment score (ES)
NES=1.50
p<0.0001
FDR q=0.028
LENGA siRNA
Control siRNA
D
KEGG Pathway Enrichment Analysis
Glutathione metabolism
p53 signaling pathway
Protein export
Antigen processing and presentation
Phagosome
Staphylococcus aureus infection
Galactose metabolism
beta−Alanine metabolism
Steroid hormone biosynthesis
Hepatitis C
0.0 0.5 1.0 1.5 2.0 2.5 3.0
−log10(Pvalue)
E
IPA Ingenuity Canonical Pathways
Aryl Hydrocarbon Receptor Signaling
Cyclins and Cell Cycle Regulation
p53 Signaling
Putrescine Degradation III
Histamine Degradation
Tryptophan Degradation X
RhoA Signaling
Cell Cycle: G1/S Checkpoint Regulation
Oxidative Ethanol Degradation III
Fatty Acid α−oxidation
0 1 2 3 4 5
-log10(Pvalue)
F
MGC-803
AGS
LENGA siRNA
siNC 1# 2#
BRD7
p53
Cyclin D1
p21
β-actin
100 kDa
55 kDa
35 kDa
25 kDa
15 kDa
40 kDa
G
MGC-803
AGS
LENGA
vector OE
BRD7
p53
p21
β-actin
100 kDa
55 kDa
25 kDa
15 kDa
40 kDa
H
siNC
LENGA siRNA 1#
LENGA siRNA 2#
vector
LENGA OE
MGC803
AGS
Relative RNA Levels
CDKN1A
TP53
BRD7
BAX
PCDH7

◂**Fig. 6** TP53 pathway is activated and induced by LENGA in GC. **A–C** GSEA was used to identify the differential signaling pathways enrichment between LENGA siRNA transfection and control in MGC803 cells. KEGG (**D**) and IPA ingenuity canonical pathways (**E**) analysis for differentially expressed genes induced by LENGA. **F** Western blotting analysis of BRD7, p53, Cyclin D1, p21 expression in MGC803 and AGS transduced with LENGA siRNA or control. **G** Western blotting analysis of BRD7, p53, p21 expression in MGC803 and AGS transduced with LENGA OE or vector. **H** Rt-PCR assays revealed the decreased expression of the cell cycle inhibitor CDKN1A and increased expression of cell–cell recognition and adhesion marker PCDH7 in MGC803 and AGS LENGA siRNA cells. In contrast, LENGA overexpression reversed the effects in both cells. BAX is an apoptosis marker involved in the TP53 pathway, but it is not regulated by BRD7/p53 complex [34]. $*P<0.05$, $**P<0.01$, $***P<0.001$

IPA upstream regulators (Fig. 4C), finding two candidate targets: bromodomain-containing protein 7 (BRD7) and RABL6, which is also known as member RAS oncogene family like 6. Through a comprehensive literature review, BRD7 aroused our interest because it played an important role in the pathophysiological processes in different types of cancers [31–33]. Therefore, it was selected for subsequent validation. Firstly, it was shown that LENGA could bind specifically to BRD7 in an RNA pull-down assay (Fig. 4D). To further substantiate this observation, RNA-binding protein immunoprecipitation (RIP) was performed with anti-BRD7 antibodies in MGC803 cell lysate, and endogenous RNAs binding to BRD7 were extracted and analyzed (Fig. 4E). PCR data showed that enrichment of LENGA in the precipitation of anti-BRD7 antibodies was greater than that of IgG, while it was similar in both groups for GAPDH (Fig. 4F).

To further determine the region in BRD7 that is required for interaction with LENGA, we performed a domain mapping assay. In vitro binding assays with a 3xFlag-BRD7 fusion protein and several deletion mutants of BRD7 (Fig. 4G). The BRD7 protein was truncated mainly into three fragments according to previous literature [31]. RIP by anti-Flag M2 affinity gel showed that LENGA interacted with the BRD7 full-length (FL), ΔC-terminal domain mutant (1–232 aa, ΔC-term), and ΔN-terminal domain mutant (136–651 aa, ΔN-term) but not with N-term (1–135 aa) and C-term (233–651 aa) (Fig. 4H, I). These results indicated that the BRD (bromodomain, 136–232 aa) of BRD7 was essential for BRD7 binding to LENGA. BRD7 usually acts as a transcriptional regulator, and previous work has shown that it interacts with TP53 and regulates the transcriptional activity of a subset of p53 target genes involved in oncogenic progression [34, 35]. We also found that TP53 was one of the most significant factors in IPA upstream regulator analysis (Table. S2), and it was detected in the RNA pull-down assay (Fig. 4D). Therefore, we wondered whether LENGA participates in the interaction between BRD7 and TP53. Co-IP confirmed that BRD7 physically interacted with TP53 (Fig. 4J); however, knockdown of LENGA dramatically reduced the binding between the two partners (Fig. 4H).

Furthermore, in order to prove the biological functions of LENGA were introduced by BRD7 through BRD domain. We constructed the BRD7 Mut plasmid which deleting the BRD domain (Fig. 4L). To minimize the effects of endogenous BRD7 in MGC803 cells, BRD7 Mut was transfected to BRD7 knockdown cells. Trans-well (Fig. 4M) and colony formation (Fig. 4N) assays revealed that both the LENGA knockdown (siLENGA) and BRD7 Mut groups had improved motility and growth ability in comparison to the control group, whereas there was no difference between the two groups themselves. The above results implied that LENGA may regulate biological functions and genes expression through BRD7.

LENGA plays an important role in the BRD7-induced modulation of chromatin accessibility to regulate gene transcription

To further address the effects of LENGA on BRD7-occupying target genes across the whole genome, we performed Cleavage Under Targets and Tagmentation (CUT&Tag) [20, 21] followed by high-throughput sequencing for BRD7 in MGC803 cells (Fig. 5A). The binding regions of BRD7 were detected in MGC803 cells. As shown in Fig. 5B, C, LENGA knockdown reduced BRD7 occupancies in DNA binding regions. Previous research has shown that BRD7 has a binding affinity for the acetylated histone ligand H3K9ac [36, 37]. We next reanalyzed the sites of H3K9ac (obtained from the GEO database) and BRD7 binding regions. The results showed that more than 69% of the regions occupied by BRD7 overlapped with those occupied by H3K9ac (Fig. 5D). A more interesting finding was that 42 genes, including CDKN1A (cyclin-dependent kinase inhibitor 1A, known as p21/WAF1, which governs cell proliferation) and PCDH7 (protocadherin 7, a marker of cell−cell recognition and adhesion, related to tumor metastasis [38]), were not only regulated by BRD7 and H3K9ac but also induced by LENGA (Fig. 5D). When LENGA was knocked down, the enrichment signals in the promoter of CDKN1A were reduced in the CUT&Tag assay (Fig. 5E and S4A), and its mRNA expression levels showed similar trends in RNA-seq (Fig. 5F). When an enrichment analysis was performed using the intersection of the BRD7- and LENGA-regulated genes by Metascape [19], it predicted that the subset of genes might be regulated by TP53 and EP300 (known as histone acetyltransferase) (Fig. S4B). To confirm the above findings in high-throughput screening, we designed three pairs of PCR primers in the region of interest. CUT&Tag PCR showed that the binding efficiency of BRD7 to the CDKN1A promoter was significantly decreased in primers 1 and 2 (Fig. 5G). A similar phenomenon was observed for

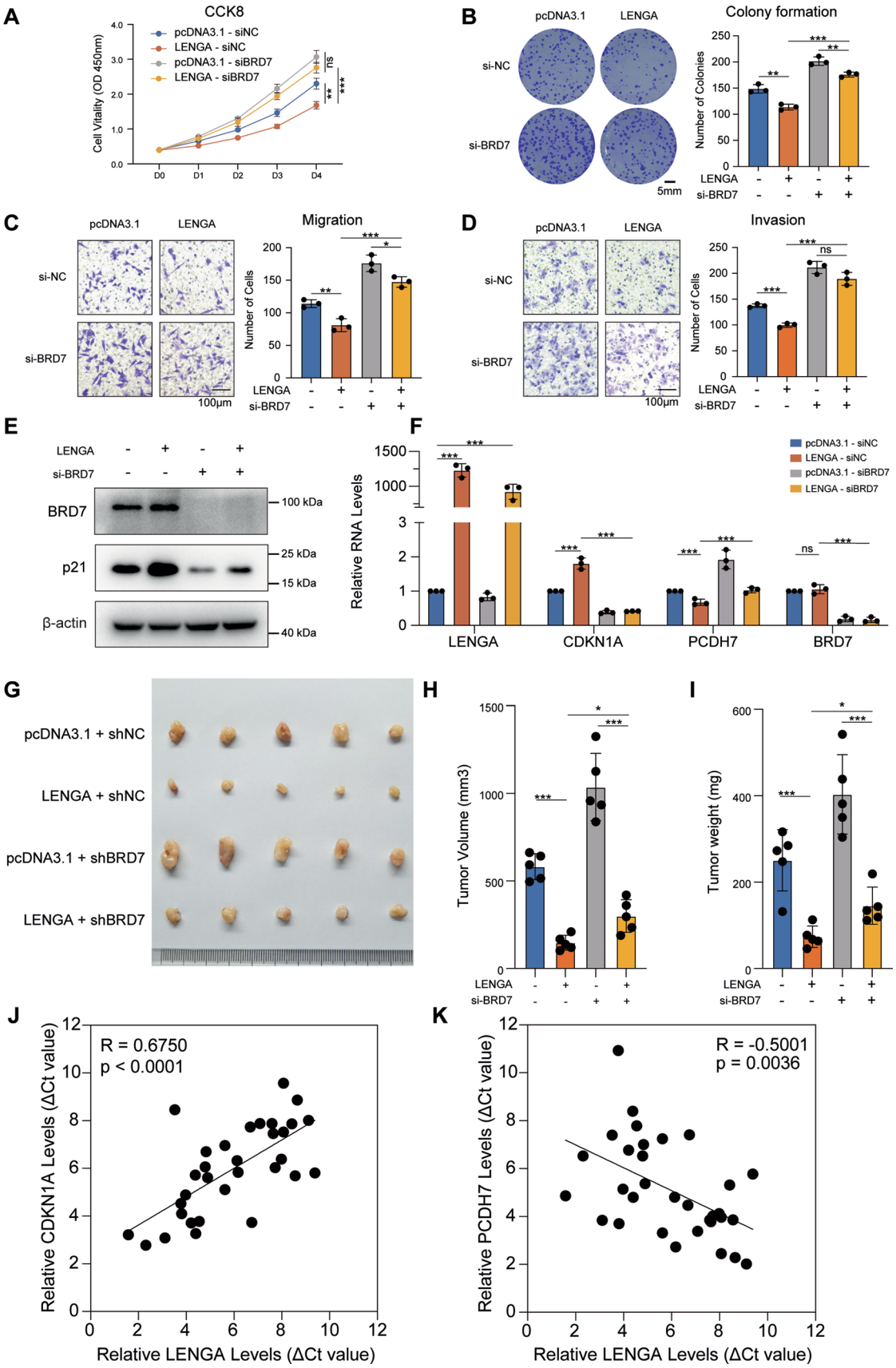
A
CCK8
pcDNA3.1 - siNC
LENGA - siNC
pcDNA3.1 - siBRD7
LENGA - siBRD7
Cell Vitality (OD 450nm)
D0
D1
D2
D3
D4
ns
**
***
B
pcDNA3.1
LENGA
si-NC
si-BRD7
5mm
Colony formation
Number of Colonies
LENGA
si-BRD7
C
Migration
Number of Cells
100μm
D
Invasion
E
BRD7
p21
β-actin
100 kDa
25 kDa
15 kDa
40 kDa
F
Relative RNA Levels
LENGA
CDKN1A
PCDH7
BRD7
G
pcDNA3.1 + shNC
LENGA + shNC
pcDNA3.1 + shBRD7
LENGA + shBRD7
H
Tumor Volume (mm3)
I
Tumor weight (mg)
J
R = 0.6750
p < 0.0001
Relative CDKN1A Levels (ΔCt value)
Relative LENGA Levels (ΔCt value)
K
R = -0.5001
p = 0.0036
Relative PCDH7 Levels (ΔCt value)
Relative LENGA Levels (ΔCt value)

◂**Fig. 7** BRD7 was necessary for LENGA-induced inhibition of malignant phenotype in GC. CCK8 assay (**A**) and colony formation assay (**B**) were used to detect the cell proliferation in MGC803 cells after different treatments. Trans-well assays were used to determine the migration (**C**) and invasion (**D**) in MGC803 cells with indicated treatment. **E** Western blotting was used to determine the expression of BRD7 and CDKN1A in MGC803 cells with the indicated treatment. **F** Rt-PCR was used to determine the expression of LENGA and other relevant mRNAs in MGC803 cells with the indicated treatment. **G** Morphological observation of xenografts in pcDNA3.1 + shNC, LENGA + shNC, pcDNA3.1 + shBRD7, and LENGA + shBRD7 groups. Tumor volume (**H**), and tumor weight (**I**) were used to evaluate the xenograft tumor. **J–K** The correlation between LENGA and CDKN1A, or PCDH7 expression was analyzed using Rt-PCR. If applicable, statistical analyses were presented on the right panel of each figure. $*P < 0.05$, $**P < 0.01$, $***P < 0.001$

PCDH7 (Figs. 5H, I, S4A). As mentioned above, we have proven that LENGA physically reinforces TP53 (a transcription factor of CDKN1A and PCDH7) and BRD7 interactions. Collectively, these data suggest that LENGA may act as a scaffold that enhances the stability of the BRD7/TP53 complex, thereby regulating histone modification recognition, target gene expression, and biological processes of GC.

LENGA inhibits GC progression in a BRD7-dependent manner

To elucidate the downstream mechanism of LENGA's function in GC, transcriptome sequencing (RNA-seq) was used to compare the gene expression profiles of LENGA short-interfering RNA (siRNA) and control siRNA transfectants. In total, 295 downregulated and 125 upregulated genes were identified (FC absolute value > 2, FDR < 0.05) after LENGA knockdown in MGC803 cells (Fig. S5A-B, Table S3). Next, we performed enrichment analysis. GSEA test showed that multiple essential molecular gene sets related to LENGA's tumor suppressor function were enriched, including the cell cycle, p53 pathway, and epithelial-mesenchymal transition (Fig. 6A–C). Kyoto Encyclopedia of Genes and Genomes (KEGG) and IPA canonical pathways showed that LENGA regulated the TP53 signaling pathway as well (Fig. 6D–E). Furthermore, several tumor-related signaling pathways were also enriched, such as glutathione metabolism, RhoA signaling, fatty acid α-oxidation, and cell cycle pathways. Western blotting showed that knockdown of LENGA increased the protein levels of p21 but had no effects on TP53 and BRD7 (Fig. 6F), while ectopic expression of LENGA downregulated p21 levels in MGC803 and AGS cells (Fig. 6G). Similarly, RT−PCR confirmed the alteration of representative genes in RNA-seq (Fig. 6H).

As we previously demonstrated, LENGA acts as a tumor suppressor gene in GC, and it mediates the interaction between BRD7 and TP53. Next, we hypothesized that BRD7 participates in the function of LENGA in GC. To test this hypothesis, we transfected BRD7 siRNA into GC cells with or without LENGA overexpression and tested its biological function. As expected, LENGA overexpression significantly inhibited proliferation and colony formation, while knockdown of BRD7 reversed the effects induced by LENGA (Fig. 7A, B). Similarly, in trans-well assays, BRD7 silencing dramatically blocked the decrease in migration and invasion ability caused by LENGA overexpression (Fig. 7C, D). Moreover, the western blot (Fig. 7E) and RT−PCR results (Fig. 7F) showed that knockdown of BRD7 reversed the increased protein and mRNA levels of p21/CDKN1A.

To ascertain in more detail whether BRD7 was accountable for the alterations in tumor growth governed by LENGA, we constructed stably transfected MGC803 cell lines with LENGA overexpression and BRD7 knockdown (LENGA + shBRD7). The pcDNA3.1 + shNC, LENGA + shNC, pcDNA3.1 + shBRD7, and LENGA + shBRD7 cells were subcutaneously injected into the flank of nude mice. As shown in Fig. 7G, the findings were consistent with the in vitro studies. LENGA significantly decreased tumor volume (Fig. 7H) and weight (Fig. 7I) as compared to negative control. However, LENGA + shBRD7 could rescue the growth inhibition induced by LENGA. These findings suggest that BRD7 participates in LENGA regulation of the growth of gastric cancer.

Next, we assessed whether LENGA expression levels are clinically correlated with CDKN1A and PCDH7 in GC patients. The abundance of CDKN1A and LENGA was detected by RT−PCR, and a positive correlation was observed in the correlation analysis (Pearson correlation coefficient $R = 0.6750$, $p < 0.0001$) (Fig. 7J). Similarly, PCDH7 was negatively correlated with LENGA expression (Pearson correlation coefficient $R = -0.5001$, $p = 0.0036$) (Fig. 7K). Taken together, these data indicated that LENGA inhibited GC progression in a BRD7-dependent manner.

Discussion

In the present study, we are the first to report and comprehensively characterize lncRNA LENGA, which acts as a tumor suppresser in human GC. Moreover, high LENGA expression in GC tissues was associated with a better prognosis and could be regarded as an independent prognostic indicator of GC (Fig. 1). LENGA inhibits gastric cell proliferation and metastasis in vitro and in vivo by activating the p53 pathway (Fig. 2, 3, 6). Mechanistically, we revealed for the first time that LENGA participates in the interaction between BRD7 and TP53 and subsequently regulates the expression of target genes, such as CDKN1A and PCDH7 (Fig. 4, 5). Moreover, BRD7 depletion relieved the inhibitory effect of malignant transformation in GC cells induced

by LENGA overexpression (Fig. 7). Taken together, our study uncovers the irreplaceable role of the novel lncRNA LENGA in inhibiting GC progression by promoting p53 pathway activation (Fig. 8).

Epigenetic modulation is one of the important hallmarks of cancer [39], including DNA methylation and histone modifications [40]. Recently, a significant focus has been placed on the role of a bromodomain-containing protein family. BRD, which consists of 110 amino acids, is a conserved structural module that can bind acetylated lysines in histone tails and regulate gene transcription by the recruitment of molecular partners [41]. BRD7, which contains one BRD, has been reported to be downregulated in many kinds of cancers, such as nasopharyngeal cancer, breast cancer, and ovarian cancer [42–44]. Our results demonstrate that BRD7 knockdown promotes GC progression, which indicates that BRD7 might also be a tumor suppressor in GC. Furthermore, BRDs have been demonstrated to recognize acetylated lysine residues. It was reported that BRD7 could bind H3K9ac [36, 37]. Our results suggest that BRD7 and H3K9ac are usually colocalized in the genome and that a subset of genes is regulated by LENGA at the same time, including CDKN1A and PCDH7. Thus, we speculate that LENGA affects the acetylation of histone lysine residues as well, which still needs further confirmation. In addition, increasing evidence has shown that BRDs can interact with noncoding RNAs, such as BRD7 with LENGA, BRD3 with DIGIT [45] and BRD4 with eRNAs [46]. The interaction often stabilizes the BRDs occupancy and activity in specific regions. Further exploration is needed to elucidate the role of lncRNAs in the recognition of acetylated histones.

Moreover, there are multiple mechanisms of the tumor suppressor BRD7 in the process of carcinogenesis. BRD7 inhibits G1-S progression through the RAS/MEK/ERK and Rb/E2F pathways [47]. With respect to tumor metastasis, BRD7 negatively regulates YB1-induced EMT [31]. BRD7 is a component of chromatin remodeling of the switch/sucrose nonfermentable (SWI/SNF) complex [11], which serves as a cofactor to regulate transcription [48, 49]. However, it remains unclear whether lncRNAs mediate its functions. LncRNAs usually exert their effects by RNA−protein interactions. In our present study, we found that LENGA physically binds with BRD7 to control gene expression and suppress the GC malignant phenotype. Interestingly, it has been reported that BRD7 interacts with the transcription factor TP53, regulating a subset of genes related to cell survival but not apoptosis [34, 35]. A similar phenomenon was observed upon LENGA knockdown; thus, we investigated the function of LENGA in the BRD7/TP53 complex. The results indicate that LENGA acts as a scaffold to strengthen the interaction between them.

Various oncogenic pathways may contribute to gastric cancer carcinogenesis [50]; however, emerging evidence has shown that lncRNAs are involved and enriched in the network of signal transduction [51]. TP53 is known as a guardian of the genome, and its cellular pathway always plays a tumor suppressor role. Therefore, understanding the mechanism of TP53 in tumor suppression is favorable for

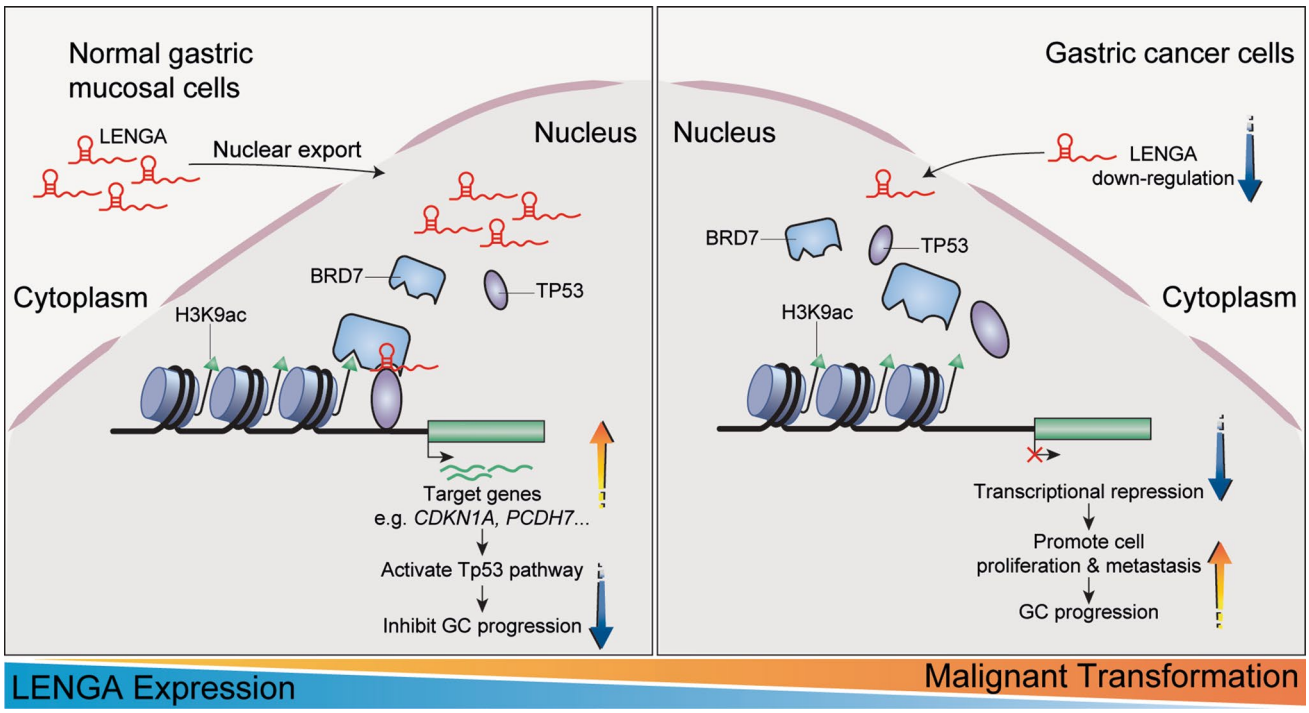

Fig. 8 A schematic diagram of the mechanism of lncRNA LENGA in GC

a potential therapy strategy. p21 is a universal cell cycle inhibitor directly controlled by TP53 and p53-dependent pathways [52]. In addition to its function in apoptosis, senescence, cell cycle arrest, and DNA repair, TP53 shows an emerging role in tumor metastasis by directly influencing the transcription of a variety of genes involved in regulating cell motility and adhesion [53], such as PCDH7 [38], which is negatively regulated by TP53 and suppresses cell migration and invasion through E-cadherin inhibition [38, 54]. Likewise, accumulating evidence suggests that lncRNAs are involved in the regulation of p53 pathway activity. The lncRNA-p21, regulated by p53, serves as a p53 corepressor, mediating the binding of heterogeneous nuclear ribonucleoprotein K (HNRNPK) and increasing the transcription of the CDKN1A gene [55]. The lncRNA GUARDIN, also regulated by p53, is sensitive to DNA damage and maintains genomic stability in multiple manners [56]. In addition, lncRNA MEG3 can regulate p53 protein stability through its E3 ubiquitin-protein ligase MDM2, subsequently regulating cell proliferation and apoptosis in a p53-dependent manner [57, 58]. In the current study, we discovered that LENGA does not affect TP53 at the mRNA and protein levels but mediates its interaction with BRD7. As a result of LENGA depletion, TP53 cannot bind to the promoter region of its target (e.g., CDKN1A). These findings highlighted that LENGA plays an important role in the regulatory network of p53.

We acknowledge some limitations in the current study. We only focused on proliferation and metastasis phenotypes in our study, and it would be interesting to determine whether LENGA is crucial in emerging fields, such as metabolism reprogramming and the tumor microenvironment. In addition, gastric cancer is highly heterogeneous, with different pathogeneses and therapeutic strategies depending on molecular characteristics. Although mutations in TP53 are most frequently observed in GC [59], investigating the mechanism of TP53 wild-type (WT) GC is equally significant. Because the cell lines used in this study are both TP53 WT, our findings may only support LENGA's role in TP53 WT GCs. More research on the function of LENGA in TP53 mutant GC is required in the future. Finally, further studies are needed to clarify whether the effects of LENGA on proliferation and metastasis are GC specific or present in other types of cancer.

Collectively, we identified a novel lncRNA, LENGA, which has low-level ectopic expression in primary tumors compared to adjacent normal tissues of GC and serves as a tumor suppressor that inhibits the proliferation and metastasis both in vitro and in vivo by scaffolding BRD7 and TP53, thereby modulating the p53 pathway and regulating the expression of CDKN1A at the transcriptional level. Furthermore, our results suggest that the aberrant LENGA expression level has prognostic value and that targeting LENGA may be pivotal in the prevention or treatment of gastric cancer.

Supplementary Information The online version contains supplementary material available at https://doi.org/10.1007/s00018-022-04642-2.

Acknowledgements This work is supported by the National Natural Science Foundation of China (NSFC) (Grant nos. 81871984, 81772831, 82072614), Advanced and Appropriate Technology Promotion Project of Shanghai Health Commission (Grant no. 2019SY030), Shanghai Municipal Key Clinical Specialty (Grant No. shslczdzk00102) and Shanghai Jiao Tong University School of Medicine "Two-hundred Talent" team (Grant no. RC20200026). We are grateful to Prof. Ming He for the discussion, and Dr. Li Xia and his team in the core facility of basic medical science (Shanghai Jiao Tong University School of Medicine) for excellent support in MS.

Author contributions Conception and design: LZ, QZ, MZ; methodology: SL, CZ, LH, SZ; acquisition of data (provided animals, acquired, and managed patients): SZ, LH, JM; analysis and interpretation of data (e.g., statistical analysis, biostatistics analysis): XY, YS, HJ, EZ; supervision: MZ, LZ; funding acquisition: LZ, QZ, MZ, JS; writing, review, or revision of the manuscript: SL, QZ, LZ, JS.

Funding This work is supported by the National Natural Science Foundation of China (NSFC) (Grant nos. 81871984, 81772831, 82072614), Advanced and Appropriate Technology Promotion Project of Shanghai Health Commission (Grant no. 2019SY030), Shanghai Municipal Key Clinical Specialty (Grant no. shslczdzk00102) and Shanghai Jiao Tong University School of Medicine "Two-hundred Talent" team (Grant no. RC20200026).

Availability of data and materials All data that support the findings of this study are available from the corresponding author upon reasonable request. High-throughput sequence data of RNA-seq and CUT&Tag was deposited in NCBI, GEO (GSE189471).

Declarations

Conflict of interest The authors have no relevant financial or non-financial interests to disclose.

Ethics approval and consent to participate The study protocol was in accordance with the guidelines set by the Ethical Committee of Ruijin Hospital. Written informed consent was obtained from all participants in the study.

Consent for publication All authors agree with the content of the manuscript.

References

1. Smyth EC, Nilsson M, Grabsch HI, van Grieken NCT, Lordick F (2020) Gastric cancer. Lancet 396(10251):635–648
2. Sung H, Ferlay J, Siegel RL, Laversanne M, Soerjomataram I, Jemal A, Bray F (2021) Global cancer statistics 2020: GLOBOCAN estimates of incidence and mortality worldwide for 36 cancers in 185 countries. CA Cancer J Clin 71(3):209–249
3. Bittoni A, Maccaroni E, Scartozzi M, Berardi R, Cascinu S (2010) Chemotherapy for locally advanced and metastatic gastric cancer: state of the art and future perspectives. Eur Rev Med Pharmacol Sci 14(4):309–314

4. Kopp F, Mendell JT (2018) Functional classification and experimental dissection of long noncoding RNAs. Cell 172(3):393–407
5. Wang KC, Chang HY (2011) Molecular mechanisms of long noncoding RNAs. Mol Cell 43(6):904–914
6. Schmitt AM, Chang HY (2016) Long noncoding RNAs in cancer pathways. Cancer Cell 29(4):452–463
7. Dragomir MP, Kopetz S, Ajani JA, Calin GA (2020) Non-coding RNAs in GI cancers: from cancer hallmarks to clinical utility. Gut 69(4):748–763
8. Sun TT, He J, Liang Q, Ren LL, Yan TT, Yu TC, Tang JY, Bao YJ, Hu Y, Lin Y et al (2016) LncRNA GClnc1 promotes gastric carcinogenesis and may act as a modular scaffold of WDR5 and KAT2A complexes to specify the histone modification pattern. Cancer Discov 6(7):784–801
9. Zhuo W, Liu Y, Li S, Guo D, Sun Q, Jin J, Rao X, Li M, Sun M, Jiang M et al (2019) Long noncoding RNA GMAN, up-regulated in gastric cancer tissues, is associated with metastasis in patients and promotes translation of ephrin A1 by competitively binding GMAN-AS. Gastroenterology 156(3):676-691e611
10. Luo Y, Zheng S, Wu Q, Wu J, Zhou R, Wang C, Wu Z, Rong X, Huang N, Sun L et al (2021) Long noncoding RNA (lncRNA) EIF3J-DT induces chemoresistance of gastric cancer via autophagy activation. Autophagy 17:1–19
11. Kaeser MD, Aslanian A, Dong MQ, Yates JR 3rd, Emerson BM (2008) BRD7, a novel PBAF-specific SWI/SNF subunit, is required for target gene activation and repression in embryonic stem cells. J Biol Chem 283(47):32254–32263
12. Levine AJ (2020) p53: 800 million years of evolution and 40 years of discovery. Nat Rev Cancer 20(8):471–480
13. Huang Y, Zhao Q, Zhou CX, Gu ZM, Li D, Xu HZ, Wiedmer T, Sims PJ, Zhao KW, Chen GQ (2006) Antileukemic roles of human phospholipid scramblase 1 gene, evidence from inducible PLSCR1-expressing leukemic cells. Oncogene 25(50):6618–6627
14. Leppek K, Stoecklin G (2014) An optimized streptavidin-binding RNA aptamer for purification of ribonucleoprotein complexes identifies novel ARE-binding proteins. Nucleic Acids Res 42(2):e13
15. Ma CN, Wo LL, Wang DF, Zhou CX, Li JC, Zhang X, Gong XF, Wang CL, He M, Zhao Q (2021) Hypoxia activated long non-coding RNA HABON regulates the growth and proliferation of hepatocarcinoma cells by binding to and antagonizing HIF-1 alpha. RNA Biol 18(11):1791–1806
16. Martin M (2011) Cutadapt removes adapter sequences from high-throughput sequencing reads. EMBnet journal 17(1):10
17. Kim D, Paggi JM, Park C, Bennett C, Salzberg SL (2019) Graph-based genome alignment and genotyping with HISAT2 and HISAT-genotype. Nat Biotechnol 37(8):907–915
18. Trapnell C, Williams BA, Pertea G, Mortazavi A, Kwan G, van Baren MJ, Salzberg SL, Wold BJ, Pachter L (2010) Transcript assembly and quantification by RNA-Seq reveals unannotated transcripts and isoform switching during cell differentiation. Nat Biotechnol 28(5):511–515
19. Zhou Y, Zhou B, Pache L, Chang M, Khodabakhshi AH, Tanaseichuk O, Benner C, Chanda SK (2019) Metascape provides a biologist-oriented resource for the analysis of systems-level datasets. Nat Commun 10(1):1523
20. Kaya-Okur HS, Wu SJ, Codomo CA, Pledger ES, Bryson TD, Henikoff JG, Ahmad K, Henikoff S (2019) CUT&Tag for efficient epigenomic profiling of small samples and single cells. Nat Commun 10(1):1930
21. Kaya-Okur HS, Janssens DH, Henikoff JG, Ahmad K, Henikoff S (2020) Efficient low-cost chromatin profiling with CUT&Tag. Nat Protoc 15(10):3264–3283
22. Zhang Y, Liu T, Meyer CA, Eeckhoute J, Johnson DS, Bernstein BE, Nusbaum C, Myers RM, Brown M, Li W et al (2008) Model-based analysis of ChIP-Seq (MACS). Genome Biol 9(9):R137
23. Ramírez F, Ryan DP, Grüning B, Bhardwaj V, Kilpert F, Richter AS, Heyne S, Dündar F, Manke T (2016) deepTools2: a next generation web server for deep-sequencing data analysis. Nucleic Acids Res 44(W1):W160–W165
24. Consortium EP (2012) An integrated encyclopedia of DNA elements in the human genome. Nature 489(7414):57–74
25. Song YX, Sun JX, Zhao JH, Yang YC, Shi JX, Wu ZH, Chen XW, Gao P, Miao ZF, Wang ZN (2017) Non-coding RNAs participate in the regulatory network of CLDN4 via ceRNA mediated miRNA evasion. Nat Commun 8(1):289
26. Fei ZH, Yu XJ, Zhou M, Su HF, Zheng Z, Xie CY (2016) Upregulated expression of long non-coding RNA LINC00982 regulates cell proliferation and its clinical relevance in patients with gastric cancer. Tumour Biol 37(2):1983–1993
27. Liu Z, Chen Z, Fan R, Jiang B, Chen X, Chen Q, Nie F, Lu K, Sun M (2017) Over-expressed long noncoding RNA HOXA11-AS promotes cell cycle progression and metastasis in gastric cancer. Mol Cancer 16(1):82
28. Gong P, Qiao F, Wu H, Cui H, Li Y, Zheng Y, Zhou M, Fan H (2018) LncRNA UCA1 promotes tumor metastasis by inducing miR-203/ZEB2 axis in gastric cancer. Cell Death Dis 9(12):1158
29. Wang L, Park HJ, Dasari S, Wang S, Kocher JP, Li W (2013) CPAT: Coding-Potential Assessment Tool using an alignment-free logistic regression model. Nucleic Acids Res 41(6):e74
30. Statello L, Guo CJ, Chen LL, Huarte M (2021) Gene regulation by long non-coding RNAs and its biological functions. Nat Rev Mol Cell Biol 22(2):96–118
31. Niu W, Luo Y, Zhou Y, Li M, Wu C, Duan Y, Wang H, Fan S, Li Z, Xiong W et al (2020) BRD7 suppresses invasion and metastasis in breast cancer by negatively regulating YB1-induced epithelial-mesenchymal transition. J Exp Clin Cancer Res 39(1):30
32. Wu WJ, Hu KS, Chen DL, Zeng ZL, Luo HY, Wang F, Wang DS, Wang ZQ, He F, Xu RH (2013) Prognostic relevance of BRD7 expression in colorectal carcinoma. Eur J Clin Invest 43(2):131–140
33. Park YA, Lee JW, Kim HS, Lee YY, Kim TJ, Choi CH, Choi JJ, Jeon HK, Cho YJ, Ryu JY et al (2014) Tumor suppressive effects of bromodomain-containing protein 7 (BRD7) in epithelial ovarian carcinoma. Clin Cancer Res 20(3):565–575
34. Drost J, Mantovani F, Tocco F, Elkon R, Comel A, Holstege H, Kerkhoven R, Jonkers J, Voorhoeve PM, Agami R et al (2010) BRD7 is a candidate tumour suppressor gene required for p53 function. Nat Cell Biol 12(4):380–389
35. Burrows AE, Smogorzewska A, Elledge SJ (2010) Polybromo-associated BRG1-associated factor components BRD7 and BAF180 are critical regulators of p53 required for induction of replicative senescence. Proc Natl Acad Sci USA 107(32):14280–14285
36. Sun H, Liu J, Zhang J, Shen W, Huang H, Xu C, Dai H, Wu J, Shi Y (2007) Solution structure of BRD7 bromodomain and its interaction with acetylated peptides from histone H3 and H4. Biochem Biophys Res Commun 358(2):435–441
37. Lloyd JT, Glass KC (2018) Biological function and histone recognition of family IV bromodomain-containing proteins. J Cell Physiol 233(3):1877–1886
38. Wei CL, Wu Q, Vega VB, Chiu KP, Ng P, Zhang T, Shahab A, Yong HC, Fu Y, Weng Z et al (2006) A global map of p53 transcription-factor binding sites in the human genome. Cell 124(1):207–219
39. Hanahan D, Weinberg RA (2011) Hallmarks of cancer: the next generation. Cell 144(5):646–674
40. Jones PA, Issa JP, Baylin S (2016) Targeting the cancer epigenome for therapy. Nat Rev Genet 17(10):630–641
41. Mita MM, Mita AC (2020) Bromodomain inhibitors a decade later: a promise unfulfilled? Br J Cancer 123(12):1713–1714

42. Harte MT, O'Brien GJ, Ryan NM, Gorski JJ, Savage KI, Crawford NT, Mullan PB, Harkin DP (2010) BRD7, a subunit of SWI/SNF complexes, binds directly to BRCA1 and regulates BRCA1-dependent transcription. Cancer Res 70(6):2538–2547
43. Chiu YH, Lee JY, Cantley LC (2014) BRD7, a tumor suppressor, interacts with p85alpha and regulates PI3K activity. Mol Cell 54(1):193–202
44. Yu X, Li Z, Shen J (2016) BRD7: a novel tumor suppressor gene in different cancers. Am J Transl Res 8(2):742–748
45. Daneshvar K, Ardehali MB, Klein IA, Hsieh F-K, Kratkiewicz AJ, Mahpour A, Cancelliere SOL, Zhou C, Cook BM, Li W et al (2020) lncRNA DIGIT and BRD3 protein form phase-separated condensates to regulate endoderm differentiation. Nat Cell Biol 6:26657
46. Rahnamoun H, Lee J, Sun Z, Lu H, Ramsey KM, Komives EA, Lauberth SM (2018) RNAs interact with BRD4 to promote enhanced chromatin engagement and transcription activation. Nat Struct Mol Biol 25(8):687–697
47. Zhou J, Ma J, Zhang BC, Li XL, Shen SR, Zhu SG, Xiong W, Liu HY, Huang H, Zhou M et al (2004) BRD7, a novel bromodomain gene, inhibits G1-S progression by transcriptionally regulating some important molecules involved in ras/MEK/ERK and Rb/E2F pathways. J Cell Physiol 200(1):89–98
48. Liu Z, Yan M, Liang Y, Liu M, Zhang K, Shao D, Jiang R, Li L, Wang C, Nussenzveig DR et al (2019) Nucleoporin Seh1 interacts with Olig2/Brd7 to promote oligodendrocyte differentiation and myelination. Neuron 102(3):587-601e587
49. Liu T, Zhao M, Liu J, He Z, Zhang Y, You H, Huang J, Lin X, Feng XH (2017) Tumor suppressor bromodomain-containing protein 7 cooperates with Smads to promote transforming growth factor-beta responses. Oncogene 36(3):362–372
50. Tan P, Yeoh KG (2015) Genetics and Molecular Pathogenesis of Gastric Adenocarcinoma. Gastroenterology 149(5):1153-1162e1153
51. Xie S, Chang Y, Jin H, Yang F, Xu Y, Yan X, Lin A, Shu Q, Zhou T (2020) Non-coding RNAs in gastric cancer. Cancer Lett 493:55–70
52. El-Deiry WS (2016) p21(WAF1) mediates cell-cycle inhibition, relevant to cancer suppression and therapy. Cancer Res 76(18):5189–5191
53. Powell E, Piwnica-Worms D, Piwnica-Worms H (2014) Contribution of p53 to metastasis. Cancer Discov 4(4):405–414
54. Chen HF, Ma RR, He JY, Zhang H, Liu XL, Guo XY, Gao P (2017) Protocadherin 7 inhibits cell migration and invasion through E-cadherin in gastric cancer. Tumour Biol 39(4):1010428317697551
55. Huarte M, Guttman M, Feldser D, Garber M, Koziol MJ, Kenzelmann-Broz D, Khalil AM, Zuk O, Amit I, Rabani M et al (2010) A large intergenic noncoding RNA induced by p53 mediates global gene repression in the p53 response. Cell 142(3):409–419
56. Hu WL, Jin L, Xu A, Wang YF, Thorne RF, Zhang XD, Wu M (2018) GUARDIN is a p53-responsive long non-coding RNA that is essential for genomic stability. Nat Cell Biol 20(4):492–502
57. Zhou Y, Zhong Y, Wang Y, Zhang X, Batista DL, Gejman R, Ansell PJ, Zhao J, Weng C, Klibanski A (2007) Activation of p53 by MEG3 non-coding RNA. J Biol Chem 282(34):24731–24742
58. Shihabudeen Haider Ali MS, Cheng X, Moran M, Haemmig S, Naldrett MJ, Alvarez S, Feinberg MW, Sun X (2019) LncRNA Meg3 protects endothelial function by regulating the DNA damage response. Nucleic Acids Res 47(3):1505–1522
59. Zang ZJ, Cutcutache I, Poon SL, Zhang SL, McPherson JR, Tao J, Rajasegaran V, Heng HL, Deng N, Gan A et al (2012) Exome sequencing of gastric adenocarcinoma identifies recurrent somatic mutations in cell adhesion and chromatin remodeling genes. Nat Genet 44(5):570–574